Available online at www.sciencedirect.com
SCIENCE DIRECT®
International Journal of Heat and Mass Transfer 48 (2005) 2090–2101
International Journal of HEAT and MASS TRANSFER
www.elsevier.com/locate/ijhmt

# Effect of variations in thermophysical properties and design parameters on the performance of a V-shaped micro grooved heat pipe

Balram Suman [a,b,*], Nazish Hoda [a]

[a] Department of Chemical Engineering and Materials Science, University of Minnesota, Minneapolis, MN 55455, USA
[b] School of Mathematics, University of Minnesota, Minneapolis, MN 55455, USA

Received 27 September 2004; received in revised form 15 January 2005
Available online 16 March 2005

**Abstract**

The paper presents a detailed simulation of a V-shaped micro heat pipe. The effect of the substrate temperature on the model has been considered. A new method for calculating dry-out length has been proposed. The sensitivity of the model to variations in thermophysical properties and design parameters has been studied. The variations in the contact angle for the substrate–coolant liquid system, surface tension and viscosity of the coolant liquid, inclination, groove angle, length of adiabatic section and radius of ungrooved substrate have been considered. The effect of design and operating parameters on the performance of the heat pipe has been studied. The variations in contact angle have been found to significantly affect the performance of a micro heat pipe. The performance of a micro heat pipe is susceptible to ungrooved area of a V-shaped micro heat pipe. If the groove is not sharp enough i.e., the radius of ungrooved substrate is more; the micro heat pipe may cease to work even before it reaches its other operating limits. The various sensitivity studies made in this work gives better understanding of variations in thermophysical properties and design parameters of a micro heat pipe.


## 1. Introduction

Micro grooved heat pipe is a reliable and efficient heat transport device and is currently an active area of research. Advances in integrated circuit technology have spurred micro heat pipe development. The current concept in integrated circuits packaging are motivated by the development of MOS and VLSI technologies, requiring higher levels of device integration. During the last thirty years, component density on integrated circuits has grown from about six thousand transistors on Intel 8080 microprocessor to over five million transistors on a similar-sized Intel P6 microprocessor. Power and component densities on these integrated circuits correlate and required power dissipation will result in increased thermal gradients and higher mean operating temperature of devices. Thus, it is necessary to develop new thermal control schemes capable of removing heat from electronic chips and reduce the mean-time-between-failure of these devices. In cases where large amounts of heat must be removed, the use of two-phase heat transfer can prove to be a wise choice. Therefore, micro

* Corresponding author. Address: Department of Chemical Engineering and Materials Science, University of Minnesota, Minneapolis, MN 55455, USA. Tel.: +1 612 625 6083; fax: +1 612 626 7246.
*E-mail address:* suman@cems.umn.edu (B. Suman).

0017-9310/$ - see front matter © 2005 Elsevier Ltd. All rights reserved.
doi:10.1016/j.ijheatmasstransfer.2005.01.007

**Nomenclature**

| | |
|---|---|
| $a$ | side length of a V-shaped groove, m |
| $A'$ | ungrooved area of substrate |
| $A_{cs}$ | area of cross section of substrate, $m^2$ |
| $A_l$ | total liquid cross-section area, $m^2$ |
| $B_1$ | constant in expression for $A_l$ |
| $B_2$ | constant in expression for $\frac{dR^*}{dX^*}$ [Eq. (3)] |
| $Cp$ | specific heat of the coolant liquid, J/(kg °C) |
| $D_h$ | hydraulic diameter, m |
| $f$ | friction factor |
| $g$ | acceleration due to gravity, $m/s^2$ |
| $K'$ | constant in expression for $B_2$ |
| $K_S$ | thermal conductivity, W/(m K) |
| $L$ | length of heat pipe, m |
| $L_h$ | half of total wetted length, m |
| $N_{Re}$ | Reynolds number |
| $P$ | liquid pressure, $N/m^2$ |
| $P^*$ | non-dimensional liquid pressure |
| $P_R$ | reference pressure, $N/m^2$ |
| $P_{v_0}$ | pressure in vapor region, $N/m^2$ |
| $Q$ | net heat flux supplied to coolant liquid, $W/m^2$ |
| $Q'$ | net heat supplied, W |
| $Q_v$ | heat flux for vaporization of liquid, $W/m^2$ |
| $R$ | radius of curvature, m |
| $R^*$ | non-dimensional radius of curvature |
| $R_0$ | reference radius of curvature, m |
| $R_l$ | meniscus surface area per unit length, m |
| $T_{con}$ | temperature at the cold end, °C |
| $T_l$ | temperature of the coolant liquid, °C |
| $T_l^*$ | dimensionless temperature of the coolant liquid |
| $T_R$ | reference temperature, °C |
| $T_S$ | temperature of substrate, °C |
| $T_S^*$ | dimensionless substrate temperature |
| $V_l$ | axial liquid velocity, m/s |
| $\lvert V_l \rvert$ | magnitude of axial liquid velocity, m/s |
| $V^*$ | non-dimensional liquid velocity |
| $V_R$ | reference liquid velocity, m/s |
| $W_b$ | groove pitch, m |
| $x$ | coordinate along the heat pipe, m |
| $X^*$ | non-dimensional coordinate along heat pipe |

*Greek symbols*

| | |
|---|---|
| $\alpha$ | half apex angle of groove, rad |
| $\beta$ | inclination of substrate with horizontal, rad |
| $\gamma$ | contact angle, rad |
| $\phi$ | curvature, $m^{-1}$ |
| $\lambda$ | latent heat of vaporization of coolant liquid, J/kg |
| $\mu_l$ | viscosity of coolant liquid, kg/m/s |
| $\rho$ | density of coolant liquid, $kg/m^3$ |
| $\sigma$ | surface tension of coolant liquid, N/m |
| $\tau_w$ | wall shear stress, $N/m^2$ |

grooved heat pipe is one of the promising options for microelectronics cooling because of its high efficiency, reliability and cost effectiveness.

Micro heat pipe, as first proposed by Cotter [1], is defined to be "so small that the mean curvature of the liquid–vapor interface is necessarily comparable in magnitude to the reciprocal of the hydraulic radius of the total flow channel." It has three sections, namely, evaporative, adiabatic and condenser. Heat input is through the evaporative section, vaporizing the coolant liquid. The vapor then passes through the adiabatic to the condenser section. In the condenser section, the vapor releases it latent heat and gets liquefied. The liquid flows towards the evaporative section, due to capillary pumping, generated by the change in the radius of curvature of the liquid meniscus. The net capillary force is generated by the combined effect of the evaporating and the condensing menisci [2]. The flow of fluid is primarily governed by the pressure jump at the liquid–vapor interface. The pressure jump at the interface is a function of the radius of curvature of the liquid meniscus, surface tension and the wettability of the coolant liquid and substrate system [3–12].

Micro heat pipes, which could be embedded directly onto the silicon substrate of an integrated circuit, have been investigated in several studies conducted by Mallik and Peterson [13,14] and Peterson et al. [15]. They have also reported experimental data taken on several water-charged micro heat pipes with a cross-sectional dimension of about one millimeter. Babin et al. [16] have also developed a steady-state micro heat pipe model to quantify heat transport capacity. Longtin et al. [17] has developed a one-dimensional steady state model of the evaporator and adiabatic sections of a micro heat pipe, which calculated working fluid pressure, velocity, and film thickness along the length of the pipe. Peterson and co-workers [16,18] have successfully used the Young–Laplace equation to describe the internal fluid dynamics of such devices. The minimum meniscus radius and the maximum heat transport in triangular grooves have also been studied [19]. A detailed thermal analysis and different limitations of a micro heat pipe have been studied by Khrustalev and Faghri [20]. Xu and Carey [21] have developed an analytical model for evaporation from a V-shaped micro groove surface assuming that the evaporation takes place only from

the thin film region of the meniscus. Ravikumar and DasGupta [22] have presented a model of evaporation from V-shaped micro grooves. Later, researchers have investigated the concept of using micro heat pipe as effective heat spreader [23,24] as well as determination of dry-out length [25,26]. Cotton and Stores [27] presented one-dimensional semi-analytical model for prediction of wetted length, supported by inclined triangular capillary groove. They have introduced the concept of accommodation theory for the change in radius of curvature at the liquid–vapor interface. Suman et al. [28] has presented a generalized model of a micro grooved heat pipe of polygonal shape. They have performed detailed study of triangular and rectangular heat pipes. They have also done transient analysis of a triangular micro grooved heat pipe [29]. Technical issues related to micro heat pipes investigated so far include liquid distribution and charge optimization [30–32], interfacial thermodynamics in micro heat pipe capillary structures [33,34] and micro heat pipe transient behavior [35]. Two reviews of micro heat pipe literature have been conducted: one by Peterson [36] and another by Cao and Faghri [37].

In this work, the existing model for a polygonal heat pipe by Suman et al. [28] has been modified for a V-shaped micro heat pipe. The boundary condition has been modified, which makes the model computationally efficient and evaluation of the dry-out length and the prediction of onset of dry-out point become easier. Additionally, substrate temperature profile has been generated and its effect on the model has been considered. The property of heat pipe to transfer heat with small temperature gradient has been studied. The developed model is capable of handling different systems e.g., any coolant liquid and substrate combination, heat flux distribution, heat input, inclination etc. The sensitivity of micro heat pipe to design and operating parameters have been studied.

## 2. Theory

A V-shaped micro grooved heat pipe is considered here. The fabrication of a very sharp apex of a groove is difficult and therefore, a roundness of an ungrooved substrate has been assumed to study the effect of roundness or ungrooved substrate on the performance of a heat pipe. The schematic of the heat pipe is shown in Fig. 1(a). The hot and the cold ends are specified as the farthest end of the evaporative and the condenser region, respectively. The heat flux absorbed/released by the liquid from the substrate in the evaporative and condenser regions is assumed to be constant although the model is capable to handle any type of heat flux distribution. Optimal amount of the coolant liquid is charged to the system so that at the steady state, the cold end remains filled with the coolant liquid, such that the radius

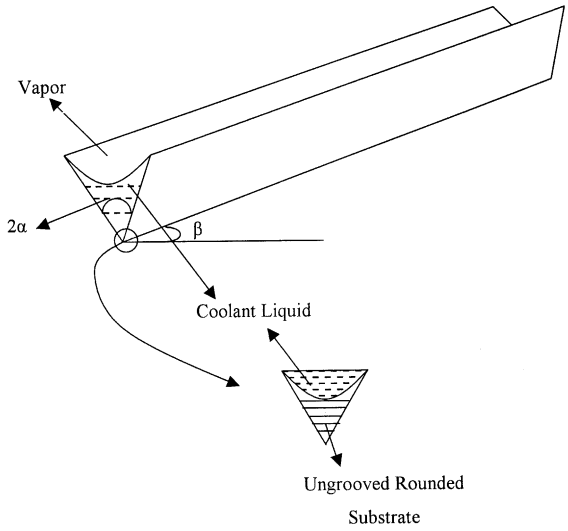


Fig. 1. Schematic of a V-shaped micro heat pipe.

of curvature can be calculated from the geometry of the system ($R = R_0$).

The modified model simulates the steady fluid flow and heat transfer, and relates them to the capillary forces present in the system using Young–Laplace equation. The model equations have been developed for all the three regions i.e., evaporative, adiabatic and condenser encompassing the complete heat pipe. The governing equations are derived under the following assumptions:

(i) one-dimensional steady incompressible flow along the length of heat pipe; (ii) negligible heat generation due to viscous dissipation; (iii) negligible flow due to surface tension; (iv) constant pressure in the vapor region in the operating range of temperature; (v) one dimensional temperature variation along the length of heat pipe; (vi) shear stress at the liquid vapor interface has been neglected; (vii) predefined heat flux distribution used by the coolant liquid and (viii) negligible convective loss.

The mass, momentum and Young–Laplace equations are taken from the previous work of Suman et al. [28]. These equations are adjusted for the V-shaped micro heat pipe and the modified geometric parameters have been presented in Appendix A. The energy balance equation for the coolant liquid has been modified. The following equation has been obtained after considering sensible heat change in the volume element (Fig. 2):

$$\rho Cp\, VA_l \frac{dT_l}{dx} = QW_b - Q_v R_l \tag{1}$$

where $Q$ is the input heat flux taken by the coolant liquid from its substrate. $Q$ is positive when added (in the evaporative section) and is negative when extracted (in the condenser region). The first term in Eq. (1) represents the sensible heat rise of the element; the heat supplied to the element is represented by the second term while

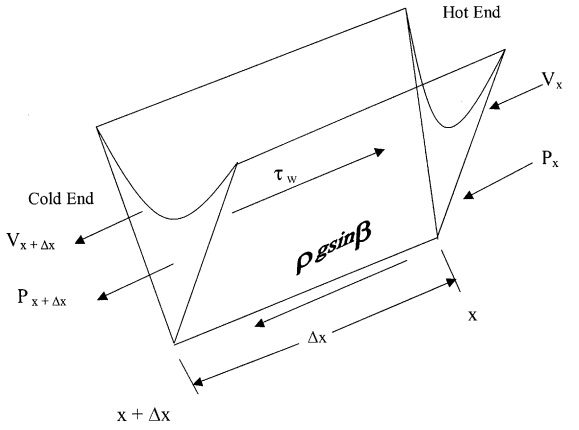


Fig. 2. Volume element of a V-shaped micro heat pipe with all forces specified.

the heat leaving the element by evaporation is given by the third term.

The steady state energy balance in the substrate is given by

$$A_{CS}K_S\frac{d^2T_S}{dx^2} - QW_b = 0 \tag{2}$$

where the first term is the net change in the conductive heat in the control volume and the second term is the heat taken up by the coolant liquid.

### 2.1. Non-dimensionalization

The modified governing equations have been non-dimensionlized choosing appropriate characteristic dimensions. The dimensional parameters have been discussed in Suman et al. [28]. The final set of non-dimensionlized equations are as follows:

$$\frac{dR^*}{dX^*} = \frac{\left[\rho g\sin(\beta) + \frac{Q_v V_R R_l V^*}{A_l \lambda} - \frac{B_2 V_R V^*}{(R_0 R^*)^2}\right]}{\left[\frac{\sigma}{R_0 L R^{*2}} - 2\rho\frac{V_R^2 V^{*2}}{L R^*}\right]} \tag{3}$$

$$\frac{dV^*}{dX^*} = -\left[\frac{Q_v R_l L}{\rho A_l \lambda V_R} + 2\frac{V^*}{R^*}\frac{dR^*}{dX^*}\right] \tag{4}$$

$$\frac{dP^*}{dX^*} = \frac{1}{R^{*2}}\frac{dR^*}{dX^*} \tag{5}$$

$$Q_v = \frac{1}{R_l}\left[QW_b - \frac{\rho Cp V_R A_l V^*}{L}\frac{dT_l}{dX^*}\right] \tag{6}$$

$$\frac{d^2T_S^*}{dX^{*2}} - \frac{Qw_b L^2}{T_R A_{CS} K_S} = 0 \tag{7}$$

where, $A_l$, $W_b$, $R_l$, $B_2$ and $B_1$ are defined in Appendix A.

Eqs. (3)–(7) are valid for all the three regions of the heat pipe namely, evaporative, adiabatic and condenser. $Q$ is zero in the adiabatic section. It is negative in the condenser region (heat is extracted) and is positive for the evaporative zone (heat is supplied). These equations have been solved numerically taking predefined heat flux distribution for the heat that is being transferred between the coolant liquid and the substrate i.e., $Q$.

### 2.2. Boundary conditions

There is no evaporation and condensation beyond the hot end ($X^* = 0$) and the cold end ($X^* = 1$) of the heat pipe, respectively. Therefore, the liquid velocity is zero at both ends of the heat pipe. The cold end is completely filled with the coolant liquid. Therefore, the radius of curvature of the liquid meniscus at the cold end ($x = L$) can be obtained from geometry and is discussed in Appendix A. The boundary conditions for substrate temperature are (i) substrate temperature at the cold end is known i.e., condenser temperature and (ii) heat input at the hot end is known. The dimensionless boundary conditions are as follows:

$$\text{at cold end}(X^* = 1), \quad R^* = 1; \quad P^* = \frac{P_{v0}}{P_R} - 1;$$
$$V^* = 0; \quad T_S^* = \frac{T_{con}}{T_R}$$

$$\text{at hot end}(X^* = 0), \quad Q_{heater} = -\frac{K_S A_{CS} T_R}{L}\left.\frac{\partial T_S^*}{\partial X^*}\right|_{X^*=0}$$

### 2.3. Numerical solution

The set of coupled ODEs (3)–(7) are model equations. They have been solved numerically. The model inputs are groove dimension, heat pipe length, $Q$ profile and thermo physical properties of coolant liquid and substrate as a function of temperature. First of all, the second-order differential equation (7) has been solved independently since it is decoupled with other equations to obtain the substrate temperature profile. Finite difference technique is used to discretize and a tridiagonal matrix has been obtained. The axial coordinate has been discretized into 40-coupled non-linear equations. The equations are further solved by using gauss–seider method. The temperature variation obtained has been used in Eqs. (3)–(6). Then, model equations (3)–(6) are solved using Runge–Kutta fourth-order integration routine. A variable step size has been taken for the above iteration with maximum step size of less than $1.0 \times 10^{-3}$. It is confirmed that the obtained result is independent of step size.

## 3. Results and discussion

The sensitive analysis of micro heat pipe using the modified model for a V-shaped heat pipe has been

presented. The silicon substrate is 0.8 cm wide and 2.3 cm long. A portion of the length, 0.3 cm, is not grooved, which is used by the heater to supply the heat to the system. Hence, the effective length of the heat pipe is 2 cm. The lengths for the evaporative, the adiabatic and the condenser regions are assumed to be equal. A V-groove width and groove spacing are taken to be 0.1 mm. Apex angle of groove is 60°. Ten such grooves have been considered in the study. The temperature at the condenser end and $T_R$ is taken as 32 °C. The inclination of the heat pipe is 10°. A constant heat flux distribution has been taken. Pentane is taken to be the working fluid and silicon as the substrate. Pentane wets silicon completely i.e., $\gamma$ (contact angle) is taken zero unless it is specified.

The substrate temperature profiles as a function of axial position for different heat inputs has been presented in Fig. 3. It has been seen that the temperature difference along the heat pipe decreases with decreases in heat input. This difference is less than one-third of the corresponding difference with the substrate of same dimensions, which looses heat only by axial conduction. For heat input of 2 W, the temperature difference with heat pipe is 1.16 °C and that with a solid substrate is 3.25 °C. It can be claimed that heat pipe can remove heat without generating much temperature difference and this property of a heat pipe makes it a promising candidate for many potential applications.

The radius of curvature has an important role in the performance of a micro grooved heat pipe. The profiles of the dimensionless radius of curvature along the length of the heat pipe ($R^*$ vs. $X^*$) for different values of heat input are presented in Fig. 4. Fig. 4 clearly shows the gradual decrease in $R^*$ as the hot end is approached signifying higher curvature at the hot end. $R^*$ at any location also decreases with increase in heat input. The behavior of the radius of curvature gives a qualitative idea of the capillary pumping. The value of $R^*$ at the hot end or the gradient $R^*$ can also predict the operating limit of a heat pipe i.e., the critical heat input for a system controlled by capillary pumping. The critical heat input for such a system, where the flow is sustained by capillary pumping, is defined as the heat input where the flow resulting from the curvature change will not be able to meet the flow requirement due to higher rates of evaporation. For such a case, the radius of curvature of the liquid meniscus at the hot end reaches a value very close to zero and the device approaches its operating limit. This limit is called capillary limit and it reaches first in many practical application. The lower limit of the radius of curvature at the onset of dry-out is taken as 0.005. Small variation in the lower limit of radius of curvature does not have significant effect on the critical heat input and the dry-out length. For the specific case considered for this study, the critical heat input is found to be 0.0115 W for an inclination of $10^0$.

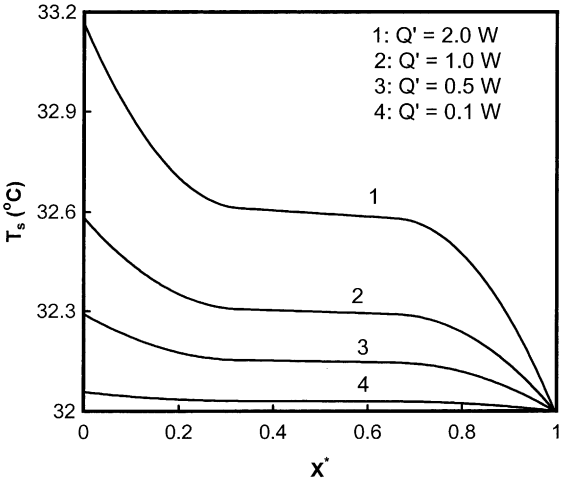


Fig. 3. Variation of substrate temperature, $T_S$ (°C) with di-mensionless position, $X^*$ with different values of heat input.

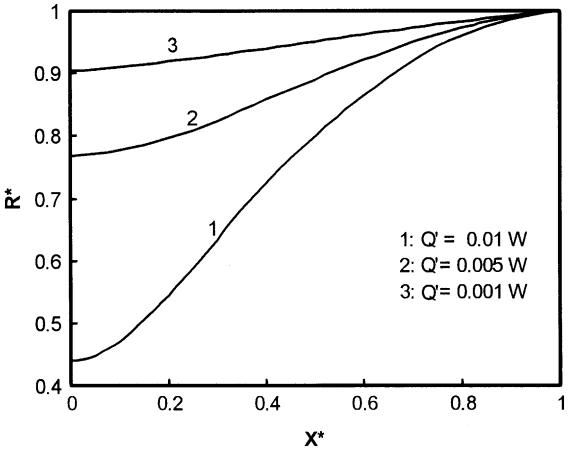


Fig. 4. Variation of dimensionless radius of curvature, $R^*$ with dimensionless position, $X^*$ with different values of heat input.

The heat pipe inclination has substantial effect on the performance of a heat pipe. The critical heat inputs, as calculated, vary significantly with inclination (Table 1). It is observed that with increase in inclination, the

Table 1
Variation of critical heat input (W) with inclination (°) for a V-shaped micro heat pipe of length 2 cm

| Inclination (°) | Critical heat input (W) × $10^2$ |
|---|---|
| 0 | 1.24 |
| 10 | 1.15 |
| 30 | 0.94 |
| 45 | 0.84 |
| 60 | 0.78 |
| 90 | 0.72 |

Table 2
Variation of critical heat input (W) with length (cm) for a V-shaped micro heat pipe of length 2 cm

| Length (cm) | Critical heat input (W) $\times 10^2$ |
|---|---|
| 1 | 2.4 |
| 2 | 1.15 |
| 3 | 0.71 |
| 4 | 0.51 |
| 5 | 0.385 |

critical heat input decreases due to the opposing (relative to capillary forces, in this configuration) effect of body force (gravity). Therefore, the capillary limit will be reached earlier for a heat pipe with a higher inclination angle. The rate of change of critical heat input w.r.t. inclination decreases with increase in inclination.

Micro heat pipe is a microscale heat transfer device. Maximum heat transport capacity of a heat pipe depends on its length. The variation of critical heat input as a function of length of a V-shaped micro heat pipe is given in Table 2. It is found that longer is the heat pipe, lesser is the critical heat input. This is because the friction loss is more in longer heat pipe. Therefore, with increase in length of a heat pipe, the performance of a heat pipe goes down. The rate of change of critical heat input w.r.t. length decreases with increase in length.

The apex angle of a V-shaped micro heat pipe plays an important role in capillary pumping. The variation of the critical heat input for a 2 cm long V-shaped micro heat pipe as a function of apex angle (and thus effectively the number of sides) is presented in Table 3. The critical heat input is found decreasing with increase in apex angle. The difference in curvature provides the capillary pumping capacity of a micro heat pipe. To pump the same amount of liquid more dimensionless curvature difference between the hot and the cold ends are required since the curvature at the cold end ($l/R_0$) decreases with increase in the apex angle. Moreover, the friction factor loss increases with apex angle. The capillary pumping capacity, therefore, decreases with increase in the apex angle.

Adiabatic section of a heat pipe can be considered as the length we want to transport the heat. The variation

Table 3
Variation of the critical heat input with groove apex angle of a V-shaped micro heat pipe of length 2 cm

| Groove apex angle (°) | Critical heat input (W) $\times 10^3$ |
|---|---|
| 40 | 12.8 |
| 60 | 11.5 |
| 80 | 7.5 |
| 120 | 1.2 |
| 150 | 0.08 |
| 160 | 0.026 |

Table 4
Variation of the critical heat input with the fraction of length as adiabatic section of a V-shaped micro heat pipe of length 2 cm

| Fraction of adiabatic length | Critical heat input (W) |
|---|---|
| 0.8 | 0.0085 |
| 0.375 | 0.010 |
| 0.33 | 0.0125 |
| 0.20 | 0.0124 |
| 0 | 0.0149 |

in critical heat input as a function of the fraction of the adiabatic length has been presented in Table 4. In this case, the length of evaporative and the condenser section have been taken to be equal and its length of a heat pipe taken to be the same. It is obtained that with increase in the fraction of the adiabatic section; the critical heat input decreases. This is because more is the adiabatic length, higher is the friction loss.

The variation of axial liquid velocity of the liquid is presented in Fig. 5. The direction of velocity is from the cold end to the hot end. Only the magnitude of the liquid velocity is considered. The absolute value of the axial liquid velocity is zero at the hot end and increases in the evaporative region. This is due to the cumulative effect of replenishing the amount evaporated throughout the evaporator region. In the adiabatic region, although there is no evaporation and condensation, the liquid velocity decreases slightly. This is because of slight increase in the radius of curvature in the adiabatic section (and hence an increase in the liquid flow area) and the friction loss. In the condenser region, there is further fall

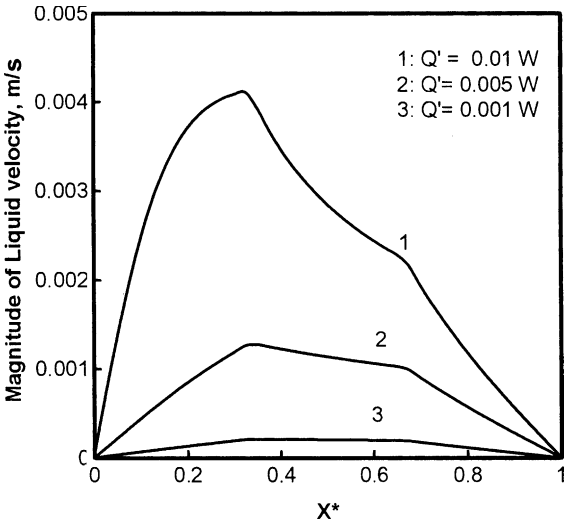


Fig. 5. Variation of magnitude of axial liquid velocity, $|V_l|$ (m/s) with dimensionless position, $X^*$ with different values of heat input.

of liquid velocity because condensation results in a sharper increase in the value of radius of curvature and finally, at the end of condenser region, the liquid velocity becomes zero. It can also be observed from the figure that with increase in heat input, evaporation increases and to replenish the enhanced amount of evaporated liquid, the velocity increases at a fixed location.

The total mass flow rate (flow rate of liquid + flow rate of vapor) at any cross section is zero. This equation gives us a vapor velocity in a heat pipe. It is important to calculate it to check the sonic limit. It is seen that the vapor velocity is much below the sonic velocity. The vapor velocity as a function of length for different heat inputs has been presented in Fig. 6. The direction of vapor velocity is from the hot end to the cold end. It has the similar trend as that of magnitude of liquid velocity in evaporative and condenser sections, which is expected. In adiabatic section, the radius of curvature increases and areas available for the liquid flow decreases. Therefore, a slight increase in vapor velocity has been obtained. But, they are opposite in direction. The magnitude of vapor velocity is more than that of liquid velocity. This is because of very low density of vapor compared to the liquid.

To sustain evaporation, liquid should flow from the cold end to the hot end. This requires the liquid pressure should decrease from the cold end to the hot end ($dP^*/dX^*$ is positive for coordinate system used herein). The variation of liquid pressure with position is presented in Fig. 7. With increase in heat input, more liquid gets evaporated in the evaporative section for evaporation. Therefore, requirement of more liquid at the evaporative section demands more pressure drop between the cold end and the hot end to sustain increase in fluid flow.

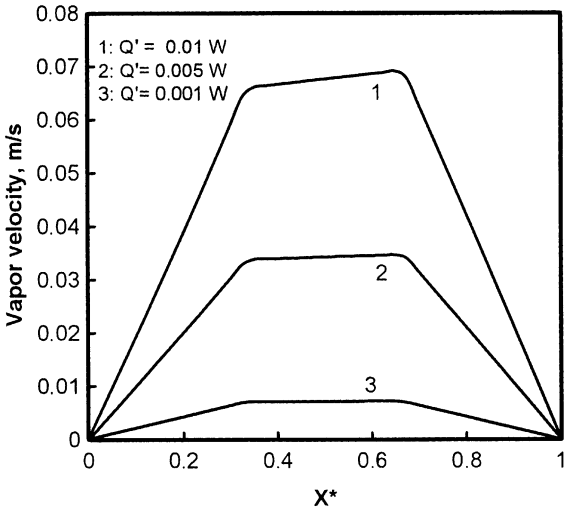


Fig. 6. Variation of axial vapor velocity, $V_g$ (m/s) with dimensionless position, $X^*$ with different values of heat input.

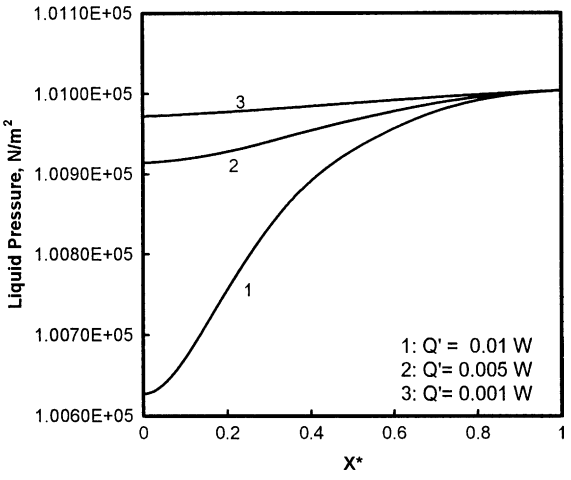


Fig. 7. Variation of liquid pressure, $P_l$ (N/m$^2$) with dimensionless position, $X^*$ with different values of heat input.

A part of the total heat supplied to the heat pipe is used by liquid to raise its temperature while remaining is used for evaporation. Only a small fraction of the heat input is used to increase the sensible heat of the liquid. It is found that the amount of heat used for sensible heat is negligible compared to the heat used for evaporation and condensation. Hence, sensible heat has negligible effect on heat pipe performance. The heat flux $Q_v$ used for evaporation of liquid as a function of position for constant heat flux distribution is presented in Fig. 8. In the evaporative region, the evaporation of coolant liquid takes place and so $Q_v$ has positive value. No evaporation and condensation take place in the adiabatic region and hence $Q_v$ is zero. In the condenser region, the condensation of the coolant liquid takes place and therefore, $Q_v$ is negative.

The effect of variation in contact angle on radius of curvature has been presented in Fig. 9. Only axial variation of curvature has been used in this study. Increase in contact angle by even one degree can give a much higher performance. More liquid can be accommodated in a smaller groove as the contact angle increases, and therefore, more liquid is available for evaporation. This increases the performance of the micro heat pipe. This finding can be used for the selection of heat pipe substrate and coolant liquid. It is advisable that the substrate and the coolant liquid combination has non-zero contact angles. By considering two dimensional curvature model, the above result for contact angle variation may change.

The effect of variation in surface tension on the radius of curvature has been presented in Fig. 10. It is obtained that with increase in surface tension of the coolant liquid, the performance of the heat pipe improves. Higher is the surface tension. More is the pressure jump at the vapor–liquid interface and therefore,

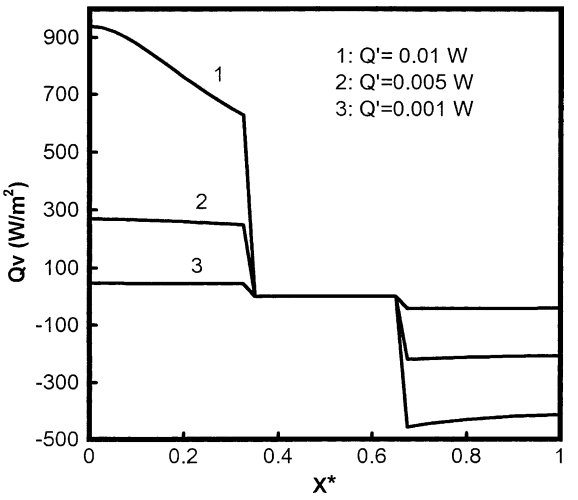


Fig. 8. Variation of evaporative heat flux $Q_v$ (W/m$^2$) with dimensionless position, $X^*$ with different values of heat input.

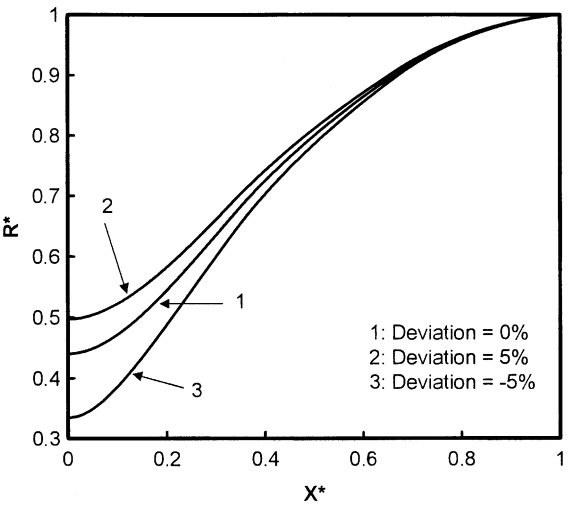


Fig. 10. Variation of dimensionless radius of curvature, $R^*$ with dimensionless position, $X^*$ with variation in surface tension.

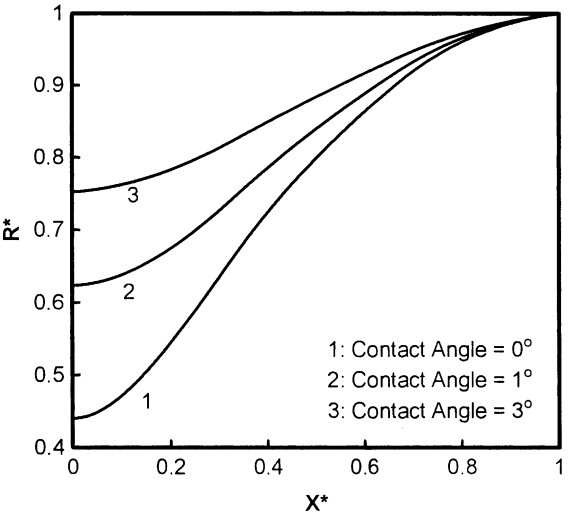


Fig. 9. Variation of dimensionless radius of curvature, $R^*$ with dimensionless position, $X^*$ with variation in contact angle.

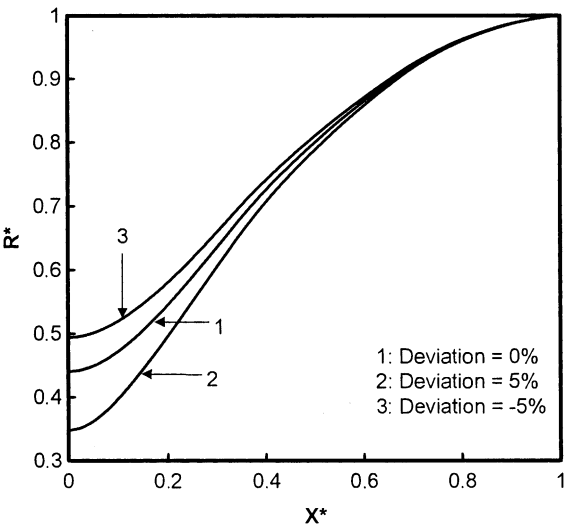


Fig. 11. Variation of dimensionless radius of curvature, $R^*$ with dimensionless position, $X^*$ with variation in viscosity.

more capillary pressure will be available to pump the liquid from the cold end to the hot end.

The effect of variation in viscosity on the radius of curvature has been presented in Fig. 11. It is obtained that with increase in viscosity of the coolant liquid, the performance of the heat pipe goes down. This is due to increase in friction loss at higher viscosity. Therefore, the performance of a heat pipe will go down.

It is well known that the surface roughness does not affect the laminar flow in macrochannels. However, as the channel size decreases to the order of few microns, the effect of surface roughness microchannels becomes important. It is said that Nusselt number and the friction factor of a high roughness microchannel increase faster than that of low roughness microchannel with increasing Reynolds number. This is because the disturbance in the boundary sub layer by the roughness is more significant at high Reynolds numbers. The design constraint restricts the fabrication of a heat pipe with very sharp corners. The corner at the vest becomes circular. An attempt has been made to capture its effect by subtracting the area of ungrooved circular section from the total available groove area. Its area is taken as a fixed percentage of the total available area for fluid flow. In Fig. 12, its effect on the radius of curvature has been shown. It is found that with increase in the ungrooved area, the performance of the heat pipe goes down. It is

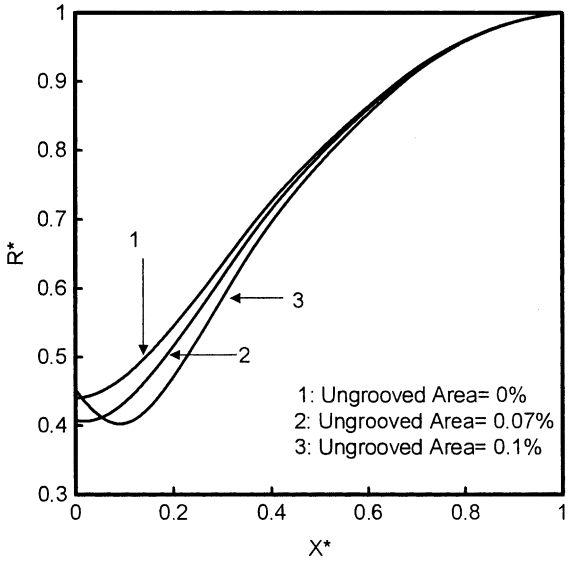


Fig. 12. Variation of dimensionless radius of curvature, $R^*$ with dimensionless position, $X^*$ with variation in radius of ungrooved rounded substrate.

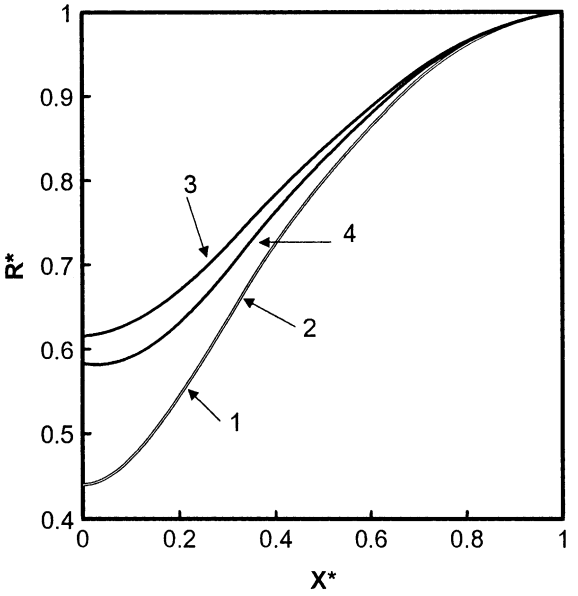


Fig. 13. Variation of dimensionless radius of curvature, $R^*$ with dimensionless position, $X^*$ with combined variation in process and design variables: (1) no variation in any variables, (2) 5% variations in surface tension and viscosity, (3) 5% variations in surface tension and viscosity and contact angle = 1°, (4) 5% variations in surface tension and viscosity and contact angle = 1° and radius of rounded ungrooved substrate is 0.01%.

expected that it would reach dry out faster and even capillary pumping would go down. But, if the ungrooved portion increases a limit, $dR^*/dX^*$ is no more monotonically increasing to provide the capillary pressure for fluid to flow from the hot end to the cold end and the heat pipe ceases to operate. From the Young–Laplace equation, it is clear that for the device to operate properly (no generation of dry spot) the radius of curvature should decrease monotonically from the cold to the hot end ($dR^*/dX^*$ should be always positive according to the coordinate system used herein). Thus, the design constraints may become the limiting operating limit of a heat pipe.

In real situation, the variations in viscosity, surface tension, contact angle etc will appear. Therefore, their combined effect has been shown in Fig. 13. They have been combined one by one. It is observed that the effect of variation in viscosity and surface tension is roughly equal. The variation in contact angle dominates the variation in surface tension and viscosity. The variation in sharpness of a corner has comparable effect.

The previous work of Ha and Peterson [25], Anand et al. [26], Suman et al. [28] for dry-out calculation is complex. The theoretical development presented herein can effectively be used to predict the onset and propagation of the dry-out length for a set of process variables. The modification in boundary condition makes is easy to handle. At the critical heat input, the radius of curvature at the hot end becomes very close to zero. Any higher value of heat input will propagate the dry region towards the cold end, as capillary pumping will not be able to sustain the increased rate of evaporation. In the dry region, coolant liquid is no more available for evaporation and hence two-phase heat transfer does not take place. The length of this region is known as dry-out length. The location of the dry-out point can be estimated numerically by calculating the value of $X^*$, where radius of curvature goes close to zero. The $X^*$ value (where, $R^* \to 0$) thus obtained, denotes the non-dimensional dry-out length of the heat pipe corresponding to the particular set of process variables. Using this methodology, the dry-out length for a V-shaped micro heat pipe has been evaluated as a function of heat input and is presented in Table 5. It can be seen from the table that the dry-out length increases with increase in heat

Table 5
Variation of dry-out length with heat input (W) of a V-shaped micro heat pipe of length 2 cm

| $Q'$ (W) | Dry out length (mm) |
|---|---|
| 0.02 | 9.0 |
| 0.03 | 11.5 |
| 0.04 | 12.7 |
| 0.05 | 13.5 |
| 0.08 | 14.9 |
| 0.1 | 15.4 |
| 0.5 | 17.9 |

input for a particular heat pipe geometry and for an inclination of $10^0$. It is found that the dry-out length calculated by the proposed method matches satisfactorily with the dry-out length obtained by Suman et al. [28], which is experimentally validated. Thus, the methodology developed herein can be effectively used to predict not only the formation of the dry region but a quantitative estimation of its propagation as well.

## 4. Conclusions

The present model for a V-shaped micro heat pipe gives a satisfactory result for heat, mass and momentum transfer coupled phenomena considered herein. An increase in the apex angle, inclination, viscosity, sharpness of the corner and length of heat pipe reduces the performance of the heat pipe. On the other hand, increase in surface tension and contact angle increases the performance. The effect of variations in contact angle, radius of rounded ungrooved substrate, apex angle and inclination are found to be prominent. To operate a heat pipe, a coolant liquid with higher surface tension, lower viscosity, higher latent heat capacity with few degree of contact angle should be preferred. The sharpness of the groove is found to be very critical. If the groove is not sharp enough i.e., the radius of ungrooved substrate is more; the heat pipe may cease to work even before it reaches its other operating limits. The developed model with modified boundary condition can easily estimate the dry-out length. The developed model can also be use to predict the onset of dry out. The present study can be extended by considering two-dimensional variations in fluid flow, heat transfer and radius of curvature, and by eliminating the predefined heat input distribution.

## Acknowledgment

The correspondence of Balram Suman with Prof. Sunando DasGupta and Prof. Sirshendu De and their valuable suggestions are gratefully acknowledged. Balram Suman would also like to thank Mr. Prabhat Kumar, Graduate Student, NCSU, USA, for critically going through the draft and his suggestions.

## Appendix A

$$R_0 = \frac{a \sin\alpha}{\cos(\alpha+\gamma)}$$

where $a$ is side length of V-shaped groove.

$W_b = 2a$

$Q = 3Q'/(W_b L)$ (for equal evaporative, adiabatic and condenser region) where $W_b$ is groove pitch.

Geometry of a V-shaped micro heat pipe is presented in Fig. A.1. The ungrooved area, $A'$ taken as a fixed percentage of a total available area. It is not shown in this Fig. A.1. Fig. 1 can be referred.

The shaded area, in Fig. A.1 is the cross-sectional area of the liquid in the heat pipe. The cross-section area of one corner is expressed as

$$A_l = \text{Area of ACBD} + \text{Area of } \triangle\text{ABC} - (\text{Area of sector AOB} - \text{Area of } \triangle\text{AOB}) - A'$$

The line diagram of section OBC in Fig. A.1 is presented in Fig. A.2 in detail. From Fig. A.2, AC and BC are the tangents to the liquid meniscus.

$$\angle\text{CAD} = \gamma$$

$$\angle\text{ADC} = \alpha$$

$$\angle\text{ACB} = 2(\alpha+\gamma)$$

$$\angle\text{AOB} = \phi = \pi - 2(\alpha+\gamma)$$

$$L_h = R\frac{\cos(\alpha+\gamma)}{\sin\alpha}$$

$$R_l = R\phi$$

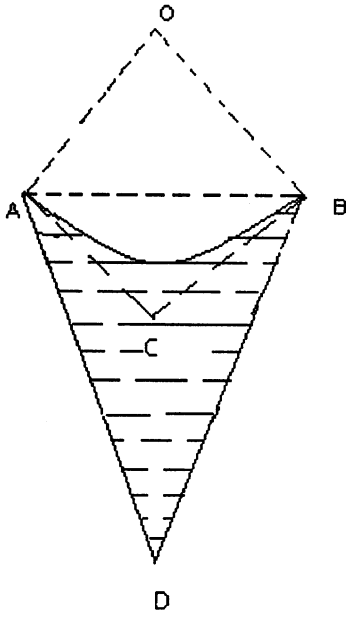


Fig. A.1. Geometry of a liquid filled corner.

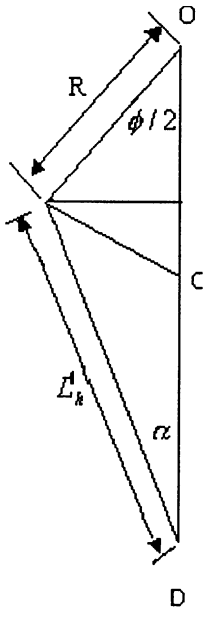


Fig. A.2. Line diagram of section OBC in Fig. A.1.

$$\text{Area of ACBD} = \frac{R^2\cot(\alpha+\gamma)\cos(\alpha+\gamma)\sin\gamma}{\sin\alpha}$$

$$\text{Area of } \triangle\text{ABC} = R^2\cot(\alpha+\gamma)\cos^2(\alpha+\gamma)$$

$$\text{Area of sector AOB} = \phi R^2/2$$

$$\text{Area of } \triangle\text{AOB} = R^2\cos(\alpha+\gamma)\sin(\alpha+\gamma)$$

Hence,

$$A_1 = R^2\left[\{\cot(\alpha+\gamma)-\varphi/2\}+\frac{\cot(\alpha+\gamma)\cos(\alpha+\gamma)\sin\gamma}{\sin\alpha}\right] - A' = B_1R^2 - A'$$

where

$$B_1 = \left[\{\cot(\alpha+\gamma)-\varphi/2\}+\frac{\cot(\alpha+\gamma)\cos(\alpha+\gamma)\sin\gamma}{\sin\alpha}\right]$$

$$B_2 = \frac{\mu_1 K'\cos^2(\alpha+\gamma)}{2\sin^2\alpha\left[\frac{\cot(\alpha+\gamma)\cos(\alpha+\gamma)\sin\gamma}{\sin\alpha}+\{\cot(\alpha+\gamma)-\varphi/2\}\right]^2}$$

## References


[1] T.P. Cotter, Principles and prospects of micro-heat pipes, in: Proceedings of the 5th Int. Heat Pipe Conference, Tsukuba, Japan, 1984, pp. 328–332.

[2] L.W. Swanson, G.C. Herdt, Model of the evaporative meniscus in a capillary tube, J. Heat Transfer 114 (1992) 434–441.

[3] S. DasGupta, J.A. Schonberg, I.Y. Kim, P.C. Wayner Jr., Use of augmented Young–Laplace equation to model equilibrium and evaporation extended menisci, J. Colloid Interf. Sci. 157 (1993) 332–342.

[4] S. DasGupta, J.A. Schonberg, P.C. Wayner Jr., Investigation of an evaporative extended meniscus based on the augmented Young–Laplace equation, J. Heat Transfer 115 (1993) 201–208.

[5] M.L. Gee, T.W. Hearly, L.R. White, Ellipsometric studies of alkenes adsorption on quartz, J. Colloid Interf. Sci. 131 (1) (1989) 18–23.

[6] S. Gokhale, J.L. Plawsky, P.C. Wayner Jr., S. DasGupta, Inferred pressure gradient and fluid flow in a condensing sessile droplet based on the measured thickness profile, Phys. Fluids 16 (6) (2004) 1942–1955.

[7] S. Moosman, S.M. Homsy, Evaporating menisci of wetting fluids, J. Colloid Interf. Sci. 73 (1980) 212–223.

[8] F. Renk, P.C. Wayner Jr., An evaporating ethanol meniscus. Part II: analytical studies, J. Heat Transfer 101 (1979) 55–62.

[9] J.G. Troung, P.C. Wayner Jr., Effects of capillary and Van der Waals dispersion forces on the equilibrium profile of a wetting liquid: theory and experimental, J. Chem. Phys. 87 (1987) 4180–4188.

[10] P.C. Wayner Jr., The effect of interfacial mass transport on flow in thin liquid films, Colloids Surf. 52 (1991) 71–84.

[11] P.C. Wayner Jr., Y.K. Kao, L.V. LaCroix, The interline heat transfer coefficient of an evaporative wetting film, Int. J. Heat Mass Transfer 19 (1976) 487–492.

[12] L. Zheng, J.L. Plawsky, P.C. Wayner Jr., S. DasGupta, Stability and oscillations in an evaporating corner meniscus, J. Heat Transfer 126 (2004) 169–178.

[13] A.K. Mallik, G.P. Peterson, Transient response characteristics of vapor deposited micro heat pipe, J. Electron. Packag. 117 (1995) 82–87.

[14] A.K. Mallik, G.P. Peterson, M.H. Weichold, On the use of micro-heat pipes as an integral part of semiconductor devices, J. Electron. Packag. 114 (1992) 436–442.

[15] G.P. Peterson, A.B. Duncan, M.H. Weichold, Experimental investigation of micro-heat pipes fabricated in silicon wafers, J. Heat Transfer 115 (1993) 751–756.

[16] B.R. Babin, G.P. Peterson, D. Wu, Steady state modeling and testing of a micro-heat pipe, J. Heat Transfer 112 (1990) 595–601.

[17] J.P. Longtin, B. Badran, F.M. Gerner, A one-dimensional model of a micro-heat pipe during steady-state operation, J. Heat Transfer 116 (1994) 709–715.

[18] D. Wu, G.P. Peterson, Investigation of the transient characteristics of a micro-heat pipe, J. Thermophys. Heat Transfer 5 (1991) 129–134.

[19] G.P. Peterson, H.B. Ma, Theoretical analysis of the maximum heat transport in triangular grooves: a study of idealized micro heat pipe, J. Heat Transfer 118 (1996) 731–739.

[20] D. Khrustalev, A. Faghri, Thermal analysis of a micro heat pipe, J. Heat Transfer 116 (1) (1994) 189–198.

[21] X. Xu, V.P. Carey, Evaporative from microgroove surface—an approximate heat transfer model and its comparison with experimental data, J. Thermophys. 4 (1990) 512–520.

[22] M. Ravikumar, S. DasGupta, Modeling of evaporation from V-shaped microgrooves, Chem. Eng. Commun. 160 (1997) 225–248.
[23] H.B. Ma, G.P. Peterson, Experimental investigation of the maximum heat transport in triangular grooves, J. Heat Transfer 118 (1996) 740–746.
[24] A.Md. Khan, S. Mishro, S. De, S. DasGupta, An experimental and theoretical investigation of evaporating cooling from V-shaped microgrooves, Int. J. Transport Phenom. 1 (1999) 277–289.
[25] J.M. Ha, G.P. Peterson, Analytical prediction of axial dry-out point for evaporating liquids in axial microgrooves, J. Heat Transfer 120 (1998) 452–457.
[26] S. Anand, S. De, S. DasGupta, Experimental and theoretical study of axial dry-out point for evaporative from V-shaped microgrooves, Int. J. Heat Mass Transfer 45 (2002) 1535–1543.
[27] I. Cotton, G.R. Stores, A semi-analytical model to predict the capillary limit of heated inclined triangular capillary grooves, J. Heat Transfer 124 (2002) 162–168.
[28] B. Suman, S. De, S. DasGupta, A model of the capillary limit of a micro grooved heat pipe and the prediction of dry out length, Int. J. Heat Fluid Flow, in press.
[29] B. Suman, S. De, S. DasGupta, Transient modeling of a micro grooved heat, Int. J. Heat Mass Transfer, in press.
[30] A.B. Duncan, G.P. Peterson, Charge optimization for a triangular-shaped etched micro heat pipe, J. Thermophys. Heat Transfer 9 (1995) 365–367.
[31] A.K. Mallik, G.P. Peterson, Steady-state investigation of vapor deposited micro heat pipe arrays, J. Electron. Packag. 117 (1995) 75–81.
[32] A.K. Mallik, G.P. Peterson, M.H. Weichold, Fabrication of vapor deposited micro heat pipe arrays as an integral part of semiconductor devices, J. Electromech. Syst. 4 (1995) 119–131.
[33] L.W. Swanson, G.P. Peterson, Interfacial thermodynamics of the capillary structures in micro heat pipes, in: F.M. Gerner, K.S. Udell (Eds.), Heat Transfer on the Microscale, vol. 253, ASME Heat Transfer Division, New York, 1993, pp. 45–51.
[34] L.W. Swanson, G.P. Peterson, Interfacial thermodynamics of micro heat pipes, J. Heat Transfer 117 (1995) 195–201.
[35] D. Wu, G.P. Peterson, W.S. Chang, Transient experimental investigation of micro heat pipes, J. Thermophys. Heat Transfer 5 (1991) 539–545.
[36] G.P. Peterson, Overview of micro heat pipe research and development, Appl. Mech. Rev. 45 (1992) 175–189.
[37] Y. Cao, A. Faghri, Micro/miniature heat pipes and operating limitations, J. Enhanced Heat Transfer 1 (1994) 265–274.